RSC Advances

ROYAL SOCIETY OF CHEMISTRY

www.rsc.org/advances

Journal Name

ARTICLE

Green synthesis of highly fluorescent AuNCs with red emission and their special sensing behavior for Al^{3+}

Dan Li, Zhenhua Chen*, Tiezhu Yang, Hao Wang, Nan Lu and Xifan Mei*

Received 00th January 20xx,
Accepted 00th January 20xx

DOI: 10.1039/x0xx00000x

www.rsc.org/

Facile methods were fabricated for preparation of highly fluorescent AuNCs with red emission using L-cysteine. Water soluble and aggregation induced AuNCs have been prepared by the empolyment of the same ligand. The emission wavelength of the as prepared water soluble AuNCs can be tuned by simply adjusting the amounts of the reactants. Interestingly，it is further found the fluorescence of AuNCs that has been quenched by Pb^{2+} can be recovered by Al^{3+}. This provides a new approach for ‘turn-on’ detection of Al^{3+} in aqueous solution. A mechanism for sensing that related to the residual reducing reagent (THPC) has been proposed base on the investigation of various related nanoclusters-based systems.

Introduction

Gold nanoclusters (AuNCs) have been developed as promising materials for various applications in recent years, due to their unique optical, electronic, and low toxic properties. [1-4] They exhibit great performance in the area of catalysis, sensing and medicine. [5-8] Though great attentions have been attracted for the application of AuNCs, the synthesis of AuNCs with bright fluorescence using cost effective protection and green ligands is still a challenge. [9] AuNCs with red emission have been obtained by using large molecules such as Bovine serum albumin (BSA) protein, Glutathione (GSH) peptide, and DNA. [10-12] However, each of them describes disadvantages. For instance, besides the expensive price and low temperature storage requirement, BSA Protein and GSH peptide require elevated temperature for the synthesis. [10, 13] Additionally, protein protected AuNCs are very difficult to be separated; DNA protected AuNCs require complicate procedures for the preparation (therefore the procedures are difficult to be repeatable). [12] Meanwhile, small molecules such as (Dihydrolipoic acid) DHLA have been employed for the preparation of AuNCs, which require simple procedures at room temperatures, but the quantum yield is quite low. [14, 15] As well as this, 11-MUA (11-Mercaptoundecanoic acid, 98%) (500 mg, ca. 400 EUR, Sigma-Aldrich) has been successfully applied for synthesis of AuNCs with red emission , [16] but the ligand is very expensive. Moreover, the excitation wavelength (ca. 300 nm, not visible) is quite short, which is not environment-friendly. Compared to these ligands, the amino acids of native protein that exists in people will provide more advantages. They are not only cost effective, but with low toxic, biocompatible, and environment-friendly properties. Until now, common amino acids of native protein such as L-histidine, L-cysteine, Methionine, and L-proline have been designed as templates for synthesis of fluorescent AuNCs with blue/green emission. [17-20] However, when these amino acids are used as templates, no fluorescent AuNCs with red emission (more environmentally friendly) have been obtained yet. For example, L-Cysteine is a market available amino acid (>99%, 1 Kg, ca. 14 EUR, alibaba), which can perform as a green ligand if AuNCs with red emission can be successfully obtained. AuNCs with green emission have been obtained by using L-Cysteine, but red emitted AuNCs hasn’t been fabricated yet. [18]

It has been reported that the composition of L-cysteine may play an important role for the culture of BSA protected AuNCs with red emission. [21, 22] In that case, tryptophan or some other amino acid may act as a weak reduction reagent. It is worth simulating a similar culture environment like BSA or other ligands where AuNCs with red emission can be found. [10] However, the reduction composition such as tryptophan of BSA is not well applied in water as a reductant by itself. When tryptophan was separated from protein, it didn’t exhibit the same performance. Thus, other weak but independent reducing reagent should be found. [23] Then, AuNCs with red emission will possibly be obtained using L-cysteine as a protection ligand.

In the case of sensing, the detection of Al^{3+} is of great importance. If high concentration of Al^{3+} is present in the environment, it will cause serious disease. [24] Fluorescent sensors have attracted interest for the detection of Al^{3+}. [25-27] Some organic sensors have been designed for detecting Al^{3+}, but these systems may bring new toxic media for aqueous solution. [28-31] The green sensing materials such as noble metal nanoclusters are expected. Recently, two methods for

Liaoning Medical University, Jinzhou, 121001, People’s Republic of China
Email: zhchen561@yahoo.com; meixifan1971@163.com
† Footnotes relating to the title and/or authors should appear here.
Electronic Supplementary Information (ESI) available: [details of any supplementary information available should be included here]. See DOI: 10.1039/x0xx00000x

determination of Al^{3+} using nanoclusters have been reported. The PEGylated MSA-AgAuNCs can be used for sensing of Al^{3+} in aqueous solution. [32] However, only 3-fold fluorescence enhancement was observed upon the addition of 2 mM of Al^{3+}. The other report found that the tyrosine-stabilized fluorescent AuNCs could be used for sensing of Al^{3+} though less than one fold enhancement was obtained. [33] In this work, we develop a facile method for synthesis of water soluble L-cysteine capped AuNCs (L-Cys-AuNCs) with bright red emission. The emission wavelength can be tuned by simply adjusting the amounts of the reactants. The protocol for synthesis is described in Scheme 1, which is similar like the culture of BSA protected AuNCs with red emission. However, our protocols are much more cost effective and the product is with high yield. It is proposed that Tetrakis(hydroxymethyl)phosphonium chloride (THPC) may play a similar role like Tryptophan or other amino acid with reducing ability of BSA.

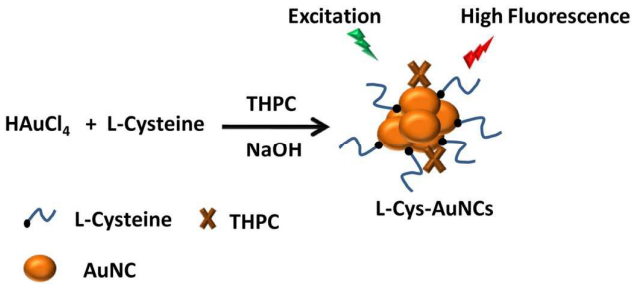

Scheme 1 Synthetic strategy for fabrication of water solubleL-Cys-AuNCs.

At the same time, a microwave assisted method was employed for the fabrication of L-Cysteine protected AuNCs with red emission (L-Cys-AuNCs-1) in the absence of additional reducing reagent. However, the as prepared AuNCs are not water soluble. Therefore, the red emission is relied on 'aggregation induced fluorescence'. [34] The protocol for the formation of L-Cys-AuNCs-1 is demonstrated in Scheme 2.

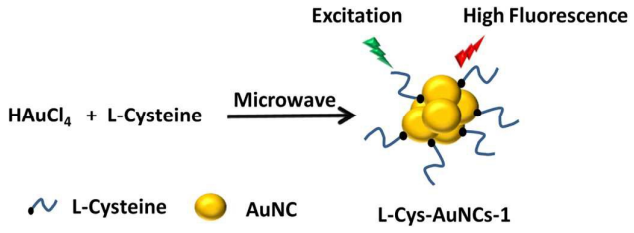

Scheme 2 Microwave assisted fabrication of L-Cys-AuNCs-1.

Furthermore, the water soluble L-Cys-AuNCs were fabricated for turn-on sensing of Al^{3+} by a special process based on the recovery of the fluorescence, which has been quenched by Pb^{2+}. To the best of our knowledge, when a common amino acid of native protein is used as a capping ligand, this is the first work that obtains AuNCs with red emission. Also, we report a first strategy for sensing of Al^{3+} based on the recovery of the fluorescence of noble metal nanoclusters that has been quenched by Pb^{2+}.

Results and discussion

To confirm the formation of the water soluble L-Cys-AuNCs, we use UV-Vis, fluorescence spectra, the comparison of photograph under dark and UV light, as well as XPS to investigate the properties (see Fig. 1). It can be seen from Fig. 1a that the synthesized L-Cys-AuNCs display a broad absorption band with a weak peak at ca. 450 nm. Just like previous AuNCs, ultra-small sizes of L-Cys-AuNCs demonstrate molecular-like properties, which are different from relatively large size gold nanoparticles. Thus, it is not surprising there is no obvious surface plasma resonance peak at 520 nm in the visible absorption region for L-Cys-AuNCs. The inset picture in Fig. 1a describes the as prepared sample under dark and UV light (365 nm UV lamp, 0.7 mW). Bright red fluorescence can be observed. On the other hand, no obvious red fluorescence can be seen by eyes using our UV lamp for some other small molecular protected AuNCs such as DHLA-AuNCs, which was reported by previous papers, though there was no big difference for their maxim excitation wavelength. [14, 35] Meanwhile, the as-prepared L-Cys-AuNCs exhibit strong red fluorescence with a maximum emission peak at ca. 700 nm under 493 nm excitation wavelength, see Fig. 1b. These results reveal the formation of L-Cys-AuNCs with bright red fluorescence. The fluorescence quantum yield was calculated at 4.3% using Acridine red (Φ_f=0.51) as a reference. Meanwhile, the emission wavelength can be tuned by adjusting the amounts of the reagents while fixing other conditions. The fluorescence emission spectra for the samples with various wavelengths are described in Fig. S1 - S3. It can be seen from Fig. S1 and Fig. S2 that the emission wavelength demonstrates red shift as a function of L-Cysteine or $HAuCl_4$. With higher concentration of either L-Cysteine or $HAuCl_4$, the forward reaction for the formation of AuNCs can proceed much faster, which enable the formation of larger sizes of AuNCs. Therefore the presence of larger size of AuNCs for the reaction product will induce the red shift of the emission wavelength. On the contrary, in the presence of more amounts of THPC, the emission wavelength demonstrates blue shift, see Fig. S3. Notwithstanding, there is no big difference for the emission wavelength when 3 - 10 μL of THPC is used. Higher concentrations of the reactant were supposed to increase the reaction rate, which should cause similar effect like higher concentration of $HAuCl_4$ and L-cysteine, but the blue shifts of the emission wavelength indicated the formation of smaller size of AuNCs. It is concluded that THPC not only acts as a reducing reagent but also it is capable of playing a role as a complexant to inhibit the reaction rate, which will be further discussed for the mechanism of sensing.

A further inspection of the composition of L-Cys-AuNCs was performed using XPS (see Fig. 1c and Fig. 1d). The valence states of the Au atoms in L-Cys-AuNCs were studied. The XPS analysis in Fig.1c reveals the Au 4f7/2 binding energy for L-Cys-AuNCs of 84.1 eV, locates between those of 84.0 eV for Au (0) and 86.0 eV for Au (I). This finding suggests that Au (0) and Au (I) species coexist in L-Cys-AuNCs. However, the binding energy describes blue shift compared to AuNCs in most papers. [36] Since the binding energy locates quite near Au (0), it indicates Au (0) plays a more important role. According to the papers, if the ratio of Au (I) was reduced to Au (0) by the introduction of $NaBH_4$, the fluorescence intensity would be significantly decreased while Au (0) played a major ratio. [37] Notwithstanding, the fluorescence is still strong for our L-Cys-AuNCs though the ratio Au (0) plays a more important role. As a result, it can be concluded that AuNCs can still exhibit bright fluorescence even though Au (I) hasn't played the major role in our case. As well as this, it can be further observed from the XPS survey (Fig. 1d) that the presence of S, N and C belongs to the L-Cysteine capping ligand. It also indicates the as prepared AuNCs are protected by L-Cysteine.

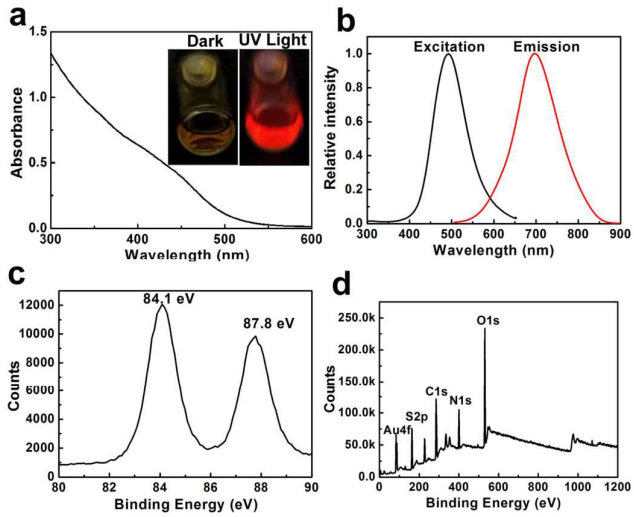

Fig. 1 Absorbance spectrum, (Inset, Photograph of L-Cys-AuNCs colloid under dark and UV light (365 nm)) (a), and fluorescence excitation, emission spectra of L-CYs–AuNCs (b); XPS analysis (Au4f) of L-CYs-AuNCs (c) and XPS survey of the L-CYs-AuNCs film (d).

As well as THPC, weather water soluble AuNCs with red emission could be obtained by using other reducing reagents was investigated, which had been often applied for the preparation of noble metal nanoclusters. For the formation of water soluble L-Cys-AuNCs with our conditions, NaOH is used to dissolve the aggregates that has been formed by the complex of L-Cysteine and gold precursor. Then, various reducing reagents have been investigated, but no fluorescent AuNCs can be found. The typical fluorescent emission spectra for the products are described in Fig. S4. It can be seen that no fluorescence but the noise signal can be detected by the instrument. At the same time, no fluorescent AuNCs can be obtained in the absence of reducing reagent either. If NaOH is not used to dissolve the aggregates between L-cysteine and gold precursor, there will be no fluorescence when no further treatment is performed, see Fig. S5a,b. According to the paper, L-cysteine is capable of acting as a reducing reagent itself to reduce Au^{3+} as Au^0, [18] but no fluorescent AuNCs are found at the current condition. It can be concluded that the ambient condition is not suitable for the formation of Au^0 to occur spontaneously. Furthermore, microwave assistance was found as a successful strategy for the formation of L-Cys-AuNCs-1 with aggregation induced red emission. The characterization for L-Cys-AuNCs-1 including photograph under visible light and UV light, UV-Vis, Fluorescence spectra, as well XPS are described in Fig. S5 – Fig. S7. Fig. S5 describes the photograph of the samples that obtained without (Fig. S5a, b) and with (Fig. S5c, d) the assistance of microwave heating. Without the assistance of microwave heating, it can be seen that the as formed colloid describe pale white colour under visible light, but no fluorescence can be seen under UV light (365 nm UV lamp, 0.7 mW). On the other hand, the as-prepared sample after microwave heating was pale white under visible light. Meanwhile, red emission under UV light can be observed, which indicates that highly fluorescent AuNCs protected by L-Cysteine (L-Cys-AuNCs-1) are formed. The maximum fluorescence intensity of L-Cys-AuNCs-1 can be obtained at 360 nm excitation wavelength, which is in consistent with the UV-vis absorption spectrum (373 nm) (Fig. S6a). As demonstrated in Fig. S6b, the maxim emission wavelength is located at 605 nm with a Stokes shift of 302 nm. The fluorescence quantum yield is calculated at 3.1% using Acridine red (Φ_f=0.51) as a reference. To further confirm the formation of L-Cys-AuNCs-1, XPS was performed. It can be seen in Fig. S7 that the Au 4f7/2 peak being at 84.5 eV indicates the valence state for Au is located between 0 and 1, which is similar to other AuNCs in most papers. [37-39] As well as this, the XPS survey indicates the presence of S, C and N, which reveals the presence of the L-Cysteine ligand. As summary, it can be concluded that the as selected reducing reagent (THPC) is of key importance for the formation of water soluble L-Cys-AuNCs at the current condition, but no additional reducing reagent is required for the formation of L-Cys-AuNCs-1 with aggregation induced emission.

Next, our samples were studied for the application as a sensor for cations. First, we performed a study for the selectivity of our L-Cys-AuNCs based sensor (S0) toward various cations, examining the properties of the designed system, see Fig. 2. As indicated in Fig. 2a, the presence of Ag^+ and Pb^{2+} resulted in quenching of the fluorescence of S0 sensor. Meanwhile, an enhancement in fluorescence was found for the sensor in the presence of Al^{3+}. In contrast, no obvious signal change occurred in the presence of other cations including Ag^+, Ba^{2+}, Ca^{2+}, Co^{2+}, Cu^{2+}, Fe^{2+}, Na^+, Ni^{2+}, NH^{4+} and Cd^{2+}.

Additionally, the sensing behaviours for Fe^{3+} and Cr^{3+} of S0 sensor are compared, which are described in Fig. S8. No

enhancement is observed like Al^{3+} though they are with the same valence states. It can be concluded that the as prepared sensor might be applied for sensing of Al^{3+}. However, according to Fig. 2b, the enhancement didn't describe great advantages over the Al^{3+} sensors in previous papers. [32] The fluorescence intensity only described 1 - 2 times enhancement and the selectivity was not excellent enough. Therefore, further fabrication was required for realizing better performance of the sensor.

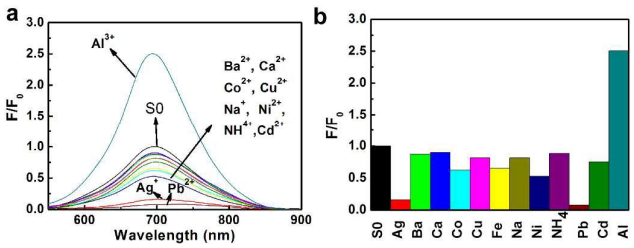

Fig. 2 Fluorescence emission spectra of L-Cys-AuNCs sensor (S0) in the presence of various metal ions (a) and the corresponding selectivity of the sensor (b). (F and F_0 are the fluorescence measured in the presence and absence of the metal ions respectively; Fe indicates Fe^{2+}).

We try to investigate whether Al^{3+} can recover the fluorescence that has been quenched by Ag^+ or Pb^{2+}. It is found that the fluorescence will no longer be enhanced in the presence of Ag^+. Based on this phenomenon, it is concluded that some chemical reaction may happen so that the decrease of the fluorescence is irreversible. For instance, Ag^+ can be reduced to Ag^0 on the surface of Au^0 by the residual adsorbed THPC. After the formation of Au-Ag, the fluorescence will be quenched due to the formation of bigger particles. In the presence of Al^{3+}, the particle cannot be recovered as fluorescent AuNCs.

On the other hand, it was found the presence of Al^{3+} can not only describe enhancement for the fluorescence of L-Cys-AuNCs based sensor, but also it can be used to recover the fluorescence that has been quenched by Pb^{2+}. Then, it was expected that much greater enhancement factor would be demonstrated if the fluorescence for the mixture of Pb^{2+} and L-Cys-AuNCs was considered as a sensing system. Then, the new sensor would be produced in the presence of Pb^{2+} and L-Cys-AuNCs (S1). As expected, we observed a much more significant enhancement factor of fluorescence in the presence of Al^{3+}, see Fig. 3. Fig. 3a describes the fluorescence emission spectra for the sensor (S0) (L-Cys-AuNCs), L-Cys-AuNCs in the presence of Pb^{2+} (S1), S1 in the presence of Al^{3+} (S1-Al), as well as S0 in the presence of Al^{3+} (S0-Al). Meanwhile, the comparison of the enhancement was demonstrated in Fig. 3b. For S0 sensor, the enhancement was ca. 1 - 2 times for Al^{3+} (S0-Al). On the other hand, if we consider S1 as the sensor, the fluorescence shows more than 14 times enhancement for sensing of Al^{3+} (S1-Al). This indicates that a highly enhancement strategy for sensing of Al^{3+} will be presented by S1 compared to S0 sensor. The enhancement is also much higher than previous papers using other nanoclusters as sensors. [32, 33] Furthermore, the corresponding pictures for the mixture of S0, S1, S1-Al, as well as S0-Al under dark and UV light are described in Fig. 3c and Fig. 3d respectively. It can be observed from Fig. 3d that there is no big difference for the comparison between S0 and S0-Al. On the other hand, obvious contrast can be seen for the comparison between S1 and S1-Al. As a result, advantages can be demonstrated by the new proposed sensing system in consideration of the enhancement and the contrast in the picture.

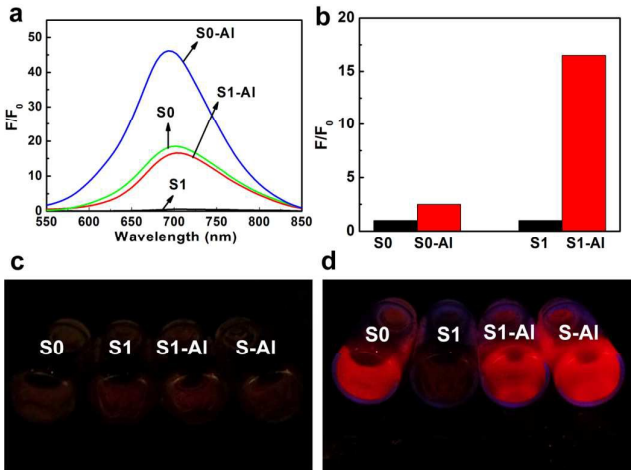

Fig. 3 Fluorescence spectra (a) of L-Cys-AuNCs sensor (S0) in the absence and presence of various metal ions such as Pb^{2+} (S1), the mixture of Pb^{2+} and Al^{3+} (S1-Al), Al^{3+} (S0-Al) and the corresponding comparisons of the sensors (b); the corresponding pictures under dark (c) and UV light (d).

Fig. 4 displays TEM images of the as-prepared L-Cys-AuNCs (S0) as well as S1, S1-Al, and S0-Al. It can be seen from Fig. 4a that the average diameter of L-Cys-AuNCs (S0) is smaller than 1 nm, as judged from image analysis of the particles. In the presence of Pb^{2+} (S1), the sizes are larger than 1 nm (Fig. 4b). This indicated the partly aggregation (soft) of the small nanoclusters, which could be caused by the complex between L-Cysteine ligand and Pb^{2+}. Notwithstanding, the aggregation is not so significant that they cannot be reversible based on the TEM image. These phenomena inspire us to develop a sensor based on the mixture of Pb^{2+} and L-Cys-AuNCs (S1). The fluorescence for the mixture of Pb^{2+} and L-Cys-AuNCs may possibly be recovered since their binding is not very strong just by complexing. In the presence of additional Al^{3+} for S1 (S1-Al), the sizes are smaller than 1 nm. In the presence of Al^{3+} for S0 (S0-Al), the sizes of the particles are also smaller than 1 nm according to the evaluation from the TEM image. It can be clearly observed from TEM that the sizes for the particles of S0 (Fig. 4a), S1-Al (Fig. 4c) and S0-Al (Fig. 4d) are small enough to describe quantum effect as well as fluorescence.

According to the TEM images, the aggregation induced enhancement is not the reason for sensing since no significant aggregation has been observed. Then, we further investigated various related systems for studying the phenomena of sensing. Since THPC was used as a reducing reagent for the preparation of water soluble L-Cys-AuNCs, it is worth investigating whether the residual THPC plays an important role for the fluorescence enhancement.

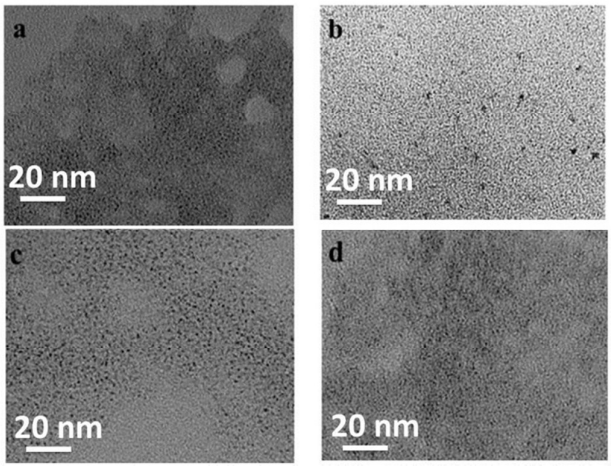

Fig. 4 TEM images of S0 (a), S1, (b), S1-Al (c), and S0-Al (d).

Initially, we study the sensing behaviour of L-Cys-AuNCs-1 where no THPC is present. The sensing behaviours including the fluorescence emission spectra in the presence of various cations and the selectivity were described in Fig. S9. It can be seen that the fluorescence is not only quenched in the presence of Ag^{+}, but also it is quenched by some other heavy cations such as Fe^{3+} and Cu^{2+}. On the other hand, there is no big difference for the intensity in the presence of Pb^{2+}. If we consider L-Cys-AuNCs-1 in the presence of Pb^{2+} as S1, the fluorescence cannot be enhanced by further addition of Al^{3+} (S1-Al). It can be concluded that the sensing behaviour for L-Cys-AuNCs-1 is quite different from that for L-Cys-AuNCs. The difference for the formation of L-Cys-AuNCs-1 is that no NaOH and THPC were used. Thus, it is worth investigating some other similar systems where both NaOH and THPC are employed. Initially, we perform similar sensing processes for AuNCs protected by L-Cysteine with using less amounts of THPC (3 μL) as reducing reagent (L-Cys-AuNCs-2). Meanwhile, several types of other metal nanoclusters that use both NaOH and THPC are also studied. The sensing behaviours for Pb^{2+}, Al^{3+}, the mixture of Pb^{2+} and Al^{3+} were studied before and after the separation of the residual THPC. The results are described in Fig. S10 - S14. Based on Fig. S3 and Fig. 1b, it is found that the emission wavelength for L-Cysteine protected AuNCs doesn't describe significant difference when 3 - 10 μL of THPC is used as the reducing reagent. Thus, it can be concluded there is no big difference for the as formed AuNCs except the amounts of the adsorbed THPC. The selectivity study for L-Cys-AuNCs-2 is described in Fig. S10. It can be seen that the fluorescence can still be quenched in the presence of Ag^{+} (Fig. S10a). However, in the presence of Pb^{2+}, the fluorescence intensity hasn't significantly decreased. Meanwhile, if we consider S0 in the presence of Pb^{2+} as another sensor (S1), the fluorescence cannot be enhanced by the further addition of Al^{3+}. For the L-Cys-AuNCs-2 sensor, only 3 μL of THPC was used. Then, less amounts of residual THPC would be adsorbed on the surface of AuNCs. As a result, it can been revealed that the residual adsorbed THPC would influence the fluorescence behaviour of the L-Cys-AuNCs in the presence of Al^{3+} since different sensing behaviors were demonstrated for L-Cys-AuNCs (10 μL), L-Cys-AuNCs-1 (0 μL) and L-Cys-AuNCs-2 (3 μL) when various amounts of THPC had been used.

After that, several kinds of AuNCs that were prepared using THPC as reducing reagent were investigated. The synthesis procedures are described by supporting information. The effect of the application of THPC was studied before and after the separation. First, Fig. S11 describes the fluorescence emission spectra of L-Cys-AuNCs in the presence of cations before and after the separation of THPC. After separation, it can be observed from Fig. S11b that the presence of Al^{3+} will partly quench the fluorescence of the purified L-Cys-AuNCs. The presence of Pb^{2+} will completely quench the fluorescence of the purified L-Cys-AuNCs. After further addition of Al^{3+} to the purified L-Cys-AuNCs-Pb^{2+} system, the fluorescence cannot be recovered. It can be seen the sensing behaviour for Al^{3+} can't be described when THPC is separated. In order to further confirm the importance of the residual THPC for sensing of Al^{3+}. Other AuNCs protected by DPA and 11-MUA were synthesized using THPC as reducing reagent. The effects of the residual THPC were also studied before and after the separation, see Fig. S12 and Fig. S13. It can be seen from Fig. S12a that the fluorescence of DPA-AuNCs is enhanced in the presence of Al^{3+}. In the presence of Pb^{2+}, the fluorescence was also quenched. Furthermore, the fluorescence of the DPA-AuNCs-Pb^{2+} system was recovered by the addition of Al^{3+}. The phenomena are quite similar to our L-Cys-AuNCs-Pb^{2+} (S1) sensing system without the purification of the residual THPC (Fig. S11a). Also, similarly, after the separation of THPC, no fluorescence enhancement can be achieved by Al^{3+} (Fig. S12b). Additionally, the 11-MUA-AuNCs system was studied (Fig. S13). It can be seen that similar phenomena happens as DPA-AuNCs and L-Cys-AuNCs based system. All the AuNCs prepared using THPC as reduction reagent have exhibited similar sensing behaviours for Al^{3+} when the residual THPC is not separated. It can be concluded that the residual THPC plays a vital role for our sensing strategy. On the other hand, we synthesized two types of AuNCs using BSA and GSH as the protection ligand without the introduction of THPC (Fig. S14). When we used the AuNCs-Pb^{2+} system as the sensor, no fluorescence enhancement would be observed in the presence of Al^{3+}. Herein, it was also confirmed that the sensing strategy couldn't be employed without using THPC as a reducing reagent. According to the results, it can be concluded that the

application of THPC as a reducing reagent plays an important role in sensing of Al^{3+}. Based on the above phenomena, the sensing process was described in Scheme 3. In the presence of Pb^{2+}, the complex between Pb^{2+} and the capping ligand (-COO) induce the quenching of the fluorescence due to the formation of 'soft' aggregation. However, since Al^{3+} has a higher binding ability with –COO in this case, after further addition of Al^{3+}, Pb^{2+} will less significantly bind with the capping ligand (-COO). Meanwhile, the complex between Al^{3+} and the adsorbed THPC can enhance the fluorescence of the L-Cys-AuNCs-Pb^{2+} (S1), which is similar to the enhancement of S0. As a result, the further addition of Al^{3+} enables the enhancement of the fluorescence that has been quenched by Pb^{2+}. This phenomenon can be employed for detection of Al^{3+}.

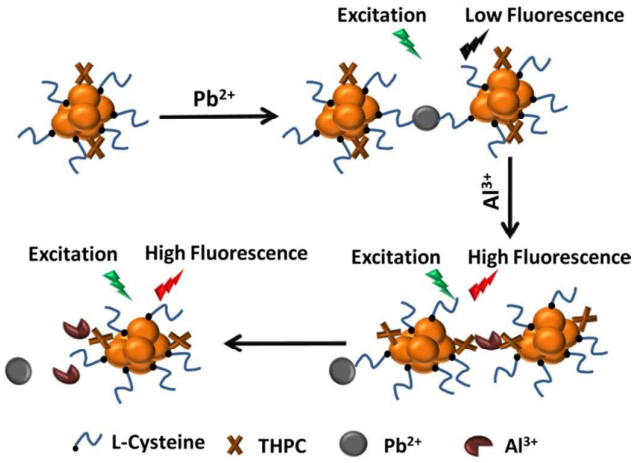

Scheme 3 Possible sensing principle of S1 for detection of Al^{3+}.

To investigate the selectivity for S1 sensing system, other cations including Ag^{+}, Ba^{2+}, Ca^{2+}, Co^{2+}, Cu^{2+}, Fe^{3+}, Na^{+}, Ni^{2+}, NH_4^{+}, Pb^{2+} and Cd^{2+} on the influence of the fluorescence at the same sensing conditions are described, see Fig. 5. The comparison for sensing of Fe^{3+} and Cr^{3+} are described in Fig. S15. The results in Fig. 5b and Fig. S15b indicate the selectivity of the S1 sensor exhibits more excellent advantages over the S0 system and previous papers. [32, 33] The corresponding pictures for the sensing systems (Fig. 5) under dark and UV light are described in Fig. S16. It can be seen that fluorescence can only be observed for S1 sensor in the presence of Al^{3+}. On the other hand, for S1 sensor in the presence of other cations, no fluorescence can be seen under the UV lamp. The high efficiency and excellent selectivity of the S1 system toward Al^{3+} suggests that our strategy is promising for the detection of selected Al^{3+} in water samples.

Furthermore, the selectivity behaviour for S1 sensor to Al^{3+} over other cations with different pH values is investigated. The results are described in Fig. S17. It can be seen the sensing behaviours are quite similar from pH4 to pH 8. However, at pH 10, the enhancement for Al^{3+} was relative low. This is possibly because the binding between Al^{3+} and THPC tend to be destroyed at high pH values.

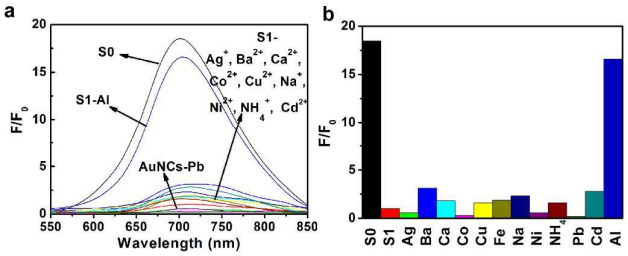

Fig. 5 Fluorescence spectra (a) of L-Cys-AuNCs-Pb^{2+} sensor (S1) in the presence of various metal ions and the corresponding selectivity (b) of the S1 sensor (Fe indicates Fe^{2+}). .

Additionally, the titration behaviour of the as prepared sensor was studied, see Fig. 6. The fluorescence turn-on spectra in Fig. 6a reveal that the fluorescence intensity of S1 sensor increased upon increasing the concentration of Al^{3+}. Fig. 6b presents the fluorescence enhancements (F/F_0) plotted with respect to the concentrations of the Al^{3+}. It is observed polynomial relationships in the ranges from 25 to 400 μM for Al^{3+} (R^2 = 0.998; $Y = -0.0000739X^2 + 0.0706X + 0.872$).

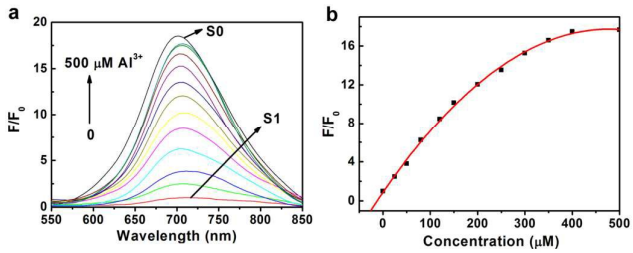

Fig. 6 Fluorescence spectra (a) of S1 probe in the presence of different concentrations of Al^{3+}; Fluorescence intensity enhancement (b) as a function of the concentration.

As well as Al^{3+}, we found some rare earth ions could be used for recovering the fluorescence that has been quenched by Pb^{2+} too. Fig. 7 describes the fluorescence of S1 in the presence of Al^{3+} as well as S1 in the presence of various rare earth cations. It can be seen that the presence of most rare earth ions with trivalent ions like Al^{3+} enable the partly recovery of the fluorescence for S1 sensing system. This is different from Fe^{3+} and Cr^{3+} since heavy metal ions tend to be quenching rather than enhancing the fluorescence of nanoclusters. Therefore, it indicated the presence of rare earth ions with comparable amounts might interfere with the detection of Al^{3+}. However, the concentration of rare earth ions in natural water is too little to compare to Al^{3+}. Still, the

proposed method can be applied in the environment. On the other hand, it can be concluded that the system might be further applied in other area based on fluorescence enhancement behaviours by the combination of rare earth.

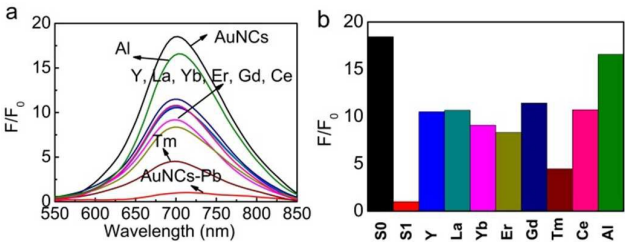

Fig. 7. (a) Fluorescence spectra of L-Cys-AuNCs-Pb^{2+}(S1) probe in the presence of different concentrations of rare earth ions and Al^{3+} (400 μM). (b) The corresponding Fluorescence enhancement (F/F0) response at 700 nm of the system to various ions. (F and F0 are the fluorescence enhancement factor measured in the absence and presence of the each metal ion).

Experimental

Reagents and instruments

All the materials for the experiments were commercially available and used as received without further purification. Tetrachloroauric-III-acid hydrate ($HAuCl_4.3H_2O$, ≥99.9%), L-Cysteine (≥97%), sodium hydroxide (NaOH, ≥98%) and Tetrakis(hydroxymethyl)phosphonium chloride solution (THPC, 80% in H_2O) and metal salts that will be used for investigating the sensing behaviours of cations were purchased from Sigma Aldrich. Metal salts are including Silver nitrate ($AgNO_3$, >99%), Barium nitrate ($Ba(NO_3)_2$, ≥99%), Calcium nitrate tetrahydrate ($Ca(NO_3)_2$, ≥99.0%), Cobalt(II) nitrate hexahydrate ($Co(NO_3)_2.6H_2O$, ≥98%), Copper(II) nitrate trihydrate ($Cu(NO_3)_2$, 98%-103%), Iron(II) sulfate heptahydrate ($FeSO_4$, 99%), Sodium sulfate anhydrous (Na_2SO_4, ≥99%), Nickel(II) nitrate hexahydrate ($Ni(NO_3)_2.6H_2O$, ≥98.5%), Ammonium chloride (NH_4Cl, 99%), Lead(II) nitrate ($Pb(NO_3)_2$, ≥99%), Cadmium nitrate tetrahydrate ($Cd(NO_3)_2.4H_2O$, ≥99.0%), Aluminum nitrate nonahydrate ($Al(NO_3)_3.9H_2O$, >99%), Chromium(III) nitrate nonahydrate ($Cr(NO_3)_3.9H_2O$, >99%), Iron(III) nitrate nonahydrate ($Fe(NO_3)_3.9H_2O$, 99.85%), Yttrium(III) nitrate hexahydrate ($Y(NO_3)_3.6H_2O$, 99.8%), Lanthanum(III) nitrate hexahydrate ($La(NO_3)_3.6H_2O$, >99%), Ytterbium(III) nitrate pentahydrate ($Yb(NO_3)_3.5H_2O$, 99.9%), Erbium(III) nitrate pentahydrate ($Er(NO_3)_3.5H_2O$, 99.9%), Gadolinium(III) nitrate hexahydrate ($Gd(NO_3)_3.6H_2O$, 99.9%), Thulium(III) nitrate pentahydrate ($Tm(NO_3)_3.6H_2O$, 99.9%), Cerium(III) nitrate hexahydrate($Ce(NO_3)_3.6H_2O$, >99.9%), were purchased from Sigma Aldrich. All the solvents were of analytical grades. Deionized water was used through the experiment. Fluorescence spectra were recorded on a FS-2 spectrophotometer (SCINCO). Transmission electron microscope (TEM) images were obtained on a Hitachi transmission electron microscope operated at 120 kV. UV-visible (UV-Vis) absorption spectra were performed on a UV-1600 spectrometer (Shangdong). X-ray photoelectron spectroscopy (XPS) spectra were obtained on Escalab 250 X-ray photoelectron spectroscope.

Preparation of L-Cys-AuNCs

In a typical procedure, 250 μL of $HAuCl_4·3H_2O$ (1%) and 5 mL of 0.1 M L-cysteine were combined in a 10 ml vial with stirring. Then, white colour aggregates were formed, but no fluorescence could be detected yet. After that, 300 μL of 1 M NaOH was combined to dissolve the aggregates. Subsequently, 10 μL of THPC (80%) was added. The solution was stirred overnight. The aqueous phase turned from colourless to bright yellow. Then, the water soluble AuNCs with red emission that are protected by L-Cysteine (L-Cys-AuNCs) are formed. For further application as sensor, the as obtained colloid will be directly used. For separation of the unreacted reactants, 10 mL of ethanol was added to 5 mL of the mixture. The yellow powder with high yield can be obtained after centrifugation at 4000 rpm. After washing the powder by ethanol-water mixture (2:1) for several times, it can be re-dispersed in water for further applications. For long term storage, the powder can be stored in refrigerator (freezing chamber), which will be stable for more than two years.
For preparation of L-Cysteine protected AuNCs with other wavelength, the conditions are kept same as the typical procedure except the mentioned parameter.

Preparation of L-Cys-AuNCs-1

In a typical procedure, freshly prepared aqueous L-cysteine (5 mL, 0.1 M) were mixed with $HAuCl_4$ (250 μL, 1%) solution in a 250 mL beaker. Under gentle stirring for 5 min, the white colour suspension was transferred to a domestic microwave oven. The irradiation time for heating was set for 30 s. After cooling down, the solution was irradiated for another 30 s. Then, the L-cysteine protected AuNCs (L-Cys-AuNCs-1) that are not soluble in water with bright red emission can be obtained. The L-Cys-AuNCs-1 can be easily precipitated and separated by centrifugation (4000 rpm).

In a typical experiment process, a 1.0 cm quartz cell was used for the fluorescence measurement. The sample was excited at 493 nm, and the emission was collected from 550 to 800 nm. The intensity was read at ca. 700 nm. 500 μL of L-Cys-AuNCs solution and 1500 μL of 1 mM of phosphate buffers buffer (pH=7) containing various concentrations of Al^{3+} were added into the quartz cell. For the selectivity experiment, other cations (400 μM) were studied in the place of Al^{3+}. For other sensing study, other AuNCs are investigated in the place of L-Cys-AuNCs with the same conditions.

Conclusions

We found facile and green approaches for the synthesis of water-soluble L-Cys-AuNCs with red emission using a common amino acid of native protein as a capping ligand. Meanwhile, a microwave assisted method for fabrication of L-Cys-AuNCs-1 with aggregation induced red emission was proposed. The water soluble L-Cys-AuNCs can be used as probes for detection of Al^{3+}. Furthermore, by the combination of Pb^{2+}, the enhancement describes advantages over the previous Al^{3+} sensor in the papers. The system can be further applied in other area based on fluorescence enhancement behaviours by the combination of rare earth ions.

Acknowledgements

This work is supported by Excellent Talents program of Liaoning Provincial Universities (No. LJQ2013089), National Natural Science Foundation of China (No. 51202199 and No. 81471854), Natural Science Foundation of Liaoning Province (No.2014022038), Liaoning Medical University Principal Fund (No. XZJJ20130104-01), Liaoning Medical University Principal Fund-Aohong Boze Students Researching Training Program (No. 2014D22) and Liaoning Provincial University Students Researching Training Programs (No. 201210160012).

Notes and references

1. C. J. Zeng, Y. X. Chen, A. Das and R. C. Jin, *J Phys Chem Lett*, 2015, **6**, 2976-2986.
2. H. Li, L. Li, A. Pedersen, Y. Gao, N. Khetrapal, H. Jonsson and X. C. Zeng, *Nano Lett*, 2015, **15**, 682-688.
3. Y. X. Chen, C. J. Zeng, D. R. Kauffman and R. C. Jin, *Nano Lett*, 2015, **15**, 3603-3609.
4. K. Pyo, V. D. Thanthirige, K. Kwak, P. Pandurangan, G. Ramakrishna and D. Lee, *J Am Chem Soc*, 2015, **137**, 8244-8250.
5. H. B. Chong and M. Z. Zhu, *Chemcatchem*, 2015, **7**, 2296-2304.
6. F. Molaabasi, S. Hosseinkhani, A. A. Moosavi-Movahedi and M. Shamsipur, *Rsc Adv*, 2015, **5**, 33123-33135.
7. L. L. Wang, J. Qiao, L. Qi, X. Z. Xu and D. Li, *Sci China Chem*, 2015, **58**, 1508-1514.
8. W. Ge, Y. Y. Zhang, J. Ye, D. H. Chen, F. U. Rehman, Q. W. Li, Y. Chen, H. Jiang and X. M. Wang, *J Nanobiotechnol*, 2015, **13**.
9. S. X. Wang, X. M. Meng, A. Das, T. Li, Y. B. Song, T. T. Cao, X. Y. Zhu, M. Z. Zhu and R. C. Jin, *Angew Chem Int Edit*, 2014, **53**, 2376-2380.
10. J. P. Xie, Y. G. Zheng and J. Y. Ying, *J Am Chem Soc*, 2009, **131**, 888-+.
11. H. Y. Zhang, Q. Liu, T. Wang, Z. J. Yun, G. L. Li, J. Y. Liu and G. B. Jiang, *Anal Chim Acta*, 2013, **770**, 140-146.
12. G. Y. Liu, Y. Shao, K. Ma, Q. H. Cui, F. Wu and S. J. Xu, *Gold Bull*, 2012, **45**, 69-74.
13. J. Zhang, Y. Yuan, G. L. Liang, M. N. Arshad, H. A. Albar, T. R. Sobahi and S. H. Yu, *Chem Commun*, 2015, **51**, 10539-10542.
14. L. Shang, L. X. Yang, F. Stockmar, R. Popescu, V. Trouillet, M. Bruns, D. Gerthsen and G. U. Nienhaus, *Nanoscale*, 2012, **4**, 4155-4160.
15. S. H. Xu, P. P. Liu, Q. W. Song, L. Wang and X. L. Luo, *Rsc Adv*, 2015, **5**, 3152-3156.
16. H. C. Chang, Y. F. Chang, N. C. Fan and J. A. A. Ho, *Acs Appl Mater Inter*, 2014, **6**, 18824-18831.
17. Y. Zhang, Q. Hu, M. C. Paau, S. P. Xie, P. F. Gao, W. Chan and M. M. F. Choi, *J Phys Chem C*, 2013, **117**, 18697-18708.
18. Y. Chen, W. Y. Li, Y. Wang, X. D. Yang, J. Chen, Y. N. Jiang, C. Yu and Q. Lin, *J Mater Chem C*, 2014, **2**, 4080-4085.
19. H. H. Deng, L. N. Zhang, S. B. He, A. L. Liu, G. W. Li, X. H. Lin, X. H. Xia and W. Chen, *Biosens Bioelectron*, 2015, **65**, 397-403.
20. X. Y. Mu, L. Qi, P. Dong, J. Qiao, J. Hou, Z. X. Nie and H. M. Ma, *Biosens Bioelectron*, 2013, **49**, 249-255.
21. Y. L. Xu, J. Sherwood, Y. Qin, D. Crowley, M. Bonizzoni and Y. P. Bao, *Nanoscale*, 2014, **6**, 1515-1524.
22. B. A. Russell, K. Kubiak-Ossowska, P. A. Mulheran, D. J. S. Birch and Y. Chen, *Phys Chem Chem Phys*, 2015, **17**, 21935-21941.
23. J. Sun, Y. Yue, P. Wang, H. L. He and Y. D. Jin, *J Mater Chem C*, 2013, **1**, 908-913.
24. A. J. Thenmozhi, T. R. W. Raja, U. Janakiraman and T. Manivasagam, *Neurochem Res*, 2015, **40**, 2006-2006.
25. A. Sahana, A. Banerjee, S. Lohar, B. Sarkar, S. K. Mukhopadhyay and D. Das, *Inorg Chem*, 2013, **52**, 3627-3633.
26. S. Goswami, K. Aich, S. Das, A. K. Das, D. Sarkar, S. Panja, T. K. Mondal and S. Mukhopadhyay, *Chem Commun (Camb)*, 2013, **49**, 10739-10741.
27. S. G. Sangita Das, Krishnendu Aich, Kakali Ghoshal, Ching Kheng Quah, Maitree Bhattacharyya and Hoong-Kun Fu, *New J Chem*, 2015, **39**, 8582-8587.
28. Y. T. Wu, Y. J. Liu, X. Gao, K. C. Gao, H. Xia, M. F. Luo, X. J. Wang, L. Ye, Y. Shi and B. Lu, *Chemosphere*, 2015, **119**, 515-523.
29. W. T. Xu, Y. F. Zhou, D. C. Huang, M. Y. Su, K. Wang and M. C. Hong, *Inorg Chem*, 2014, **53**, 6497-6499.
30. C. H. Chen, D. J. Liao, C. F. Wan and A. T. Wu, *The Analyst*, 2013, **138**, 2527-2530.
31. O. Alici and S. Erdemir, *Sensors and Actuators B: Chemical*, 2015, **208**, 159-163.
32. T. Y. Zhou, L. P. Lin, M. C. Rong, Y. Q. Jiang and X. Chen, *Anal Chem*, 2013, **85**, 9839-9844.
33. X. Y. Mu, L. Qi, J. Qiao and H. M. Ma, *Anal Methods-Uk*, 2014, **6**, 6445-6451.
34. Z. T. Luo, X. Yuan, Y. Yu, Q. B. Zhang, D. T. Leong, J. Y. Lee and J. P. Xie, *J Am Chem Soc*, 2012, **134**, 16662-16670.
35. L. Shang, N. Azadfar, F. Stockmar, W. Send, V. Trouillet, M. Bruns, D. Gerthsen and G. U. Nienhaus, *Small*, 2011, **7**, 2614-2620.
36. D. P. Anderson, J. F. Alvino, A. Gentleman, H. Al Qahtani, L. Thomsen, M. I. J. Polson, G. F. Metha, V. B. Golovko and G. G. Andersson, *Phys Chem Chem Phys*, 2013, **15**, 3917-3929.
37. C. Zhou, C. Sun, M. X. Yu, Y. P. Qin, J. G. Wang, M. Kim and J. Zheng, *J Phys Chem C*, 2010, **114**, 7727-7732.
38. X. J. Tu, W. B. Chen and X. Q. Guo, *Nanotechnology*, 2011, **22**.

39. X. Le Guevel, B. Hotzer, G. Jung, K. Hollemeyer, V. Trouillet and M. Schneider, *J Phys Chem C*, 2011, **115**, 10955-10963.

Green synthesis of highly fluorescent AuNCs with red emission and their special sensing behavior for Al^{3+}

Dan Li, Zhenhua Chen*, Tiezhu Yang, Hao Wang, Nan Lu and Xifan Mei*